Emerging Topics in Life Sciences (2018)
https://doi.org/10.1042/ETLS20170163

Review Article

On the edge of exceptional preservation: insights into the role of redox state in Burgess Shale-type taphonomic windows from the Mural Formation, Alberta, Canada

Erik A. Sperling[1], Uwe Balthasar[2] and Christian B. Skovsted[3]

[1]Department of Geological Sciences, Stanford University, Stanford, CA 94305, U.S.A.; [2]School of Geography, Earth and Environmental Sciences, University of Plymouth, PL4 8AA Plymouth, U.K.; [3]Department of Palaeobiology, Swedish Museum of Natural History, Box 50007, SE-104 05 Stockholm, Sweden

Correspondence: Erik A. Sperling (esper@stanford.edu)

Animals originated in the Neoproterozoic and 'exploded' into the fossil record in the Cambrian. The Cambrian also represents a high point in the animal fossil record for the preservation of soft tissues that are normally degraded. Specifically, fossils from Burgess Shale-type (BST) preservational windows give paleontologists an unparalleled view into early animal evolution. Why this time interval hosts such exceptional preservation, and why this preservational window declines in the early Paleozoic, have been long-standing questions. Anoxic conditions have been hypothesized to play a role in BST preservation, but recent geochemical investigations of these deposits have reached contradictory results with respect to the redox state of overlying bottom waters. Here, we report a multi-proxy geochemical study of the Lower Cambrian Mural Formation, Alberta, Canada. At the type section, the Mural Formation preserves rare recalcitrant organic tissues in shales that were deposited near storm wave base (a Tier 3 deposit; the worst level of soft-tissue preservation). The geochemical signature of this section shows little to no evidence of anoxic conditions, in contrast with published multi-proxy studies of more celebrated Tier 1 and 2 deposits. These data help confirm that 'decay-limited' BST biotas were deposited in more oxygenated conditions, and support a role for anoxic conditions in BST preservation. Finally, we discuss the role of iron reduction in BST preservation, including the formation of iron-rich clays and inducement of sealing seafloor carbonate cements. As oceans and sediment columns became more oxygenated and more sulfidic through the early Paleozoic, these geochemical changes may have helped close the BST taphonomic window.

Introduction

The Cambrian radiation of animal life represents the appearance of nearly every major animal phylum in the fossil record within a geologically rapid span of ~25 million years. The rapid increase in animal diversity and disparity is apparent in multiple records including the normal shelly fossil record (e.g. brachiopods and trilobites; [1]), the trace fossil record [2–4], phosphatized small shelly fossils [5–7] and small carbonaceous fossils [8,9]. The most celebrated archive of this event, though, is from Burgess Shale-type (BST) deposits, where primary organic tissues are preserved as thin carbonaceous films (see ref. [10] for definitions). Critically, these Lagerstätten preserve the soft parts of animals, and while the communities do not preserve a completely unbiased snapshot of early Cambrian life (for instance, size; [11]), they do provide our best glimpse of early metazoan ecosystems

Received: 5 March 2018
Revised: 22 May 2018
Accepted: 25 May 2018

Version of Record published: 26 July 2018

Emerging Topics in Life Sciences (2018)
https://doi.org/10.1042/ETLS20170163

[12–15]. Most important, by preserving most or all characters of an organism, fossils from BST biotas have been critical in understanding the polarity and order of morphological character evolution within each individual phylum [16].

The question of how organisms can escape the decay process and why these BST Lagerstätten appear to be concentrated in the Cambrian period — even after accounting for factors like rock outcrop area [17,18] — has long intrigued geologists. It was recognized early on that low-oxygen levels (or complete anoxia) might play a prominent role in reducing decay. Actualistic decay experiments, however, established that decay under anoxic conditions (at least in the presence of normal marine sulfate levels) can still proceed rapidly [19,20]. For soft-bodied deposits in general, then, anoxia mainly serves to (1) prevent scavenging, which would otherwise destroy carcasses [21], and (2) help induce the precipitation of authigenic minerals, which are involved in most exceptionally preserved deposits [22]. In the most recent review of BST preservation [10], the window for abundant and exquisite BST fossil preservation is hypothesized to occur in a 'goldilocks' zone near where the chemocline (the point in the water column at which no oxygen remains) intersects the seafloor. At seafloor depths well below the chemocline, the setting is 'supply-limited' in that animals cannot live in anoxic conditions, and carcasses simply cannot be supplied to these preservational settings through transport. Only preservation of nektonic/planktonic organisms falling through the water column could potentially occur. Conversely, at seafloor depths well above the chemocline, the setting is 'decay-limited' (preservation-limited) in that aerobic degradation and bioturbating organisms quickly destroy carcasses. Gaines [10] directly related the quality of preservation and species-level diversity of BST biotas to the position of these deposits along the spectrum from 'supply-limited' to 'decay-limited'. The most spectacular deposits, such as the Burgess Shale and Chengjiang (Tier 1), are hypothesized to occur in the window where there is sufficient transport energy to carry soft-bodied benthic organisms across the chemocline into anoxic waters. Tier 2 deposits such as Kaili, Marjum, and Spence lack sufficient transport energy or have source communities too far up-slope above the chemocline, and hence, it is hydrodynamically light organisms (e.g. algae) or dead carcasses that are dominantly carried to the zone of exceptional preservation. Conversely, the labile tissues of organisms living *in situ* in these up-slope communities are only rarely preserved due to the prevalence of more oxygenated conditions. Thus, at different points along a water-depth transect, these Tier 2 deposits are both supply- and decay-limited. Tier 3 deposits such as Latham or Indian Springs are hypothesized to have been deposited near storm wave base in relatively oxygenated conditions, and soft tissues are almost completely decomposed. Or in another sense, only the most recalcitrant tissues are preserved (e.g. [23]). These Tier 3 sites are consequently the most 'decay-limited' in this classification scheme.

This hypothesized relationship between BST preservation and the chemocline [10] has mainly been developed on the basis of sedimentological and ichnological data (e.g. [24]). To test this framework, in recent years geochemists have applied several tools to the question, most notably iron speciation analysis and the study of redox-sensitive trace metal concentrations. Both of these proxies rely on identifying enrichments of specific phases or elements (that are known to be incorporated into sediments under reducing conditions) relative to average crustal values or empirically determined shale baselines. Iron speciation tracks the ratio of total iron (FeT) to highly reactive iron phases (FeHR; iron in pyrite plus those iron phases reactive with sulfide on early diagenetic timescales, including iron oxides, iron carbonates and magnetite). In the modern ocean, sediment samples deposited beneath an oxygenated water column have FeHR/FeT <0.38 [25,26]. Samples deposited beneath an anoxic water column generally have ratios >0.38, although rapid deposition, for instance in turbidites, can mute enrichments (the lowest modern anoxic samples have ratios as low as 0.20; [25,27]). Critically, this proxy can also distinguish different types of anoxic water columns: between anoxic and ferruginous water columns (those with free ferrous iron, or more specifically not enough sulfide production to titrate available reactive iron), and anoxic and euxinic water columns (with free sulfide). This is accomplished by examining the proportion of reactive iron that has been pyritized (FeP; represents iron in pyrite). Generally, anoxic samples with FeP/FeHR >0.7–0.8 are interpreted as euxinic, with ratios below this interpreted as ferruginous [26]. As discussed below, whether a water column was ferruginous versus euxinic has important implications for interpreting trace metal patterns, and, perhaps, BST preservation itself.

Analysis of redox-sensitive trace metal concentrations relies on the observation that these elements (such as molybdenum, uranium, vanadium or chromium) are generally soluble in oxygenated water columns, and become insoluble and form complexes with organic matter, sulfides, or other mineral phases upon reduction in suboxic (only trace amounts of oxygen present; ~0.1 ml/l) or anoxic (zero oxygen) water columns [28]. Such authigenic metal enrichments are identifiable by comparing concentrations in a given shale sample against

baselines meant to represent the background detrital input, such as world shale average [29] or average upper continental crust [30]. Concentrations above these baselines would point toward authigenic enrichment and, by inference, a reducing water column. Like with iron speciation, rapid deposition will result in less time for authigenic enrichments to accumulate.

The sequestration pathways for each element are unique, with different reducing conditions and the presence/absence of sulfide having large effects on the level of enrichment. For instance, sulfide levels >11 μM are required for the quantitative switch from molybdate anion to tetrathiomolybdate, which increases particle reactivity and hence the removal of Mo from the water column into the sediment [31,32]. Vanadium does not require sulfidic conditions for initial reduction, but also undergoes a second reduction step in the presence of significant sulfide levels [33], and the presence of large sedimentary V enrichments may require sulfide. Historically, most of the research on authigenic metal enrichment has focused on modern systems or Mesozoic Ocean Anoxic Events, both of which are characterized by water columns and sediments that were generally sulfidic when anoxic. However, ferruginous conditions are increasingly being identified throughout pre-Mesozoic oceans [26,34–36], and recent debate has focused on expected metal enrichments under such conditions [27,37–40]. Although this debate remains open with respect to the exact magnitude of enrichment expected, studies have agreed that redox-sensitive metal enrichments will be relatively muted in ancient ferruginous settings. Further complicating the picture, two elements whose enrichment does not depend on the strict presence of sulfide — vanadium and chromium — are the redox-sensitive metals most influenced by variations in the detrital fraction, making the detection of muted enrichments difficult [28,41].

Redox studies of BST deposits

Analyses using iron speciation and some studies of redox-sensitive metal concentrations have provided contrasting interpretations of redox state during deposition of BST deposits. Consistent with a role for anoxia in the preservational model, iron speciation analyses of the Series 3 Wheeler Shale, Utah, have indicated a mixture of ferruginous and oxic conditions ([35,42]; although note that no data to date have been presented in a stratigraphic or paleontological context). An iron speciation and trace metal abundance investigation of the Series 2 Chengjiang Lagerstätte, South China, revealed euxinic conditions stratigraphically beneath the exceptionally preserved deposits, followed by the development of more 'equivocal' conditions in the zone of exceptional preservation [43]. Specifically, FeP/FeHR ratios were <0.7, and FeHR/FeT ratios were between 0.2 and 0.38, which in combination with low Mo concentration and in the context of the turbiditic setting, could indicate either an oxic or ferruginous water column [43,44]. Nitrogen isotopes were also investigated in these Chengjiang cores and showed a more readily interpretable signal. Hammarlund et al. [43] suggested, based on positive nitrogen isotope values, that the water column was strongly denitrifying (similar to the cores of modern oxygen minimum zones; OMZs) above the zone of exceptional preservation. Overall, these data point toward 'suboxic' to anoxic (but non-sulfidic) conditions during deposition of the Chengjiang BST deposits. Echoing these results, a detailed multi-proxy study of the Series 2 Sirius Passet deposit in North Greenland reported transiently anoxic (ferruginous) conditions during the interval of highest soft-bodied fossil abundance and diversity [45].

In contrast, trace metal data from these and other BST deposits have been interpreted as indicative of oxygenated conditions at the seafloor. Near-crustal levels of redox-sensitive metals (e.g. Mo, U, V and Cr) have been found in the Burgess Shale itself [46], Chengjiang ([42,43]; though higher abundances were found in the lower Maotianshan Shale), Sirius Passet [47], Emu Bay Lagerstätte in South Australia [48], the Rockslide Formation in northwestern Canada [49], the Wheeler and Spence shales in Utah [44] and the Indian Springs Lagerstätte, Nevada [50]. These relatively low enrichments have generally been interpreted as representing a purely detrital trace metal source and an oxygenated water column. Consequently, it has also been inferred that anoxia did not play a role (or was not required) for BST preservation. In some cases, the robustness of these trace metal signals has been questioned because several deposits (such as the Burgess Shale and Sirius Passet) have experienced considerable metamorphism [24]. However, given the consistent and widespread pattern in deposits with lower metamorphic grade, this is probably a primary depositional signature. But while probably primary, the common interpretative paradigm that low redox-sensitive trace metal contents indicate oxygenated conditions (e.g. Jones and Manning [51]) was developed prior to our current understanding that anoxic but non-sulfidic (ferruginous) water columns — with low trace metal enrichments compared with euxinic systems — are common in the geological record. Given this new framework, these published trace metal data provide no evidence for euxinic conditions, but they are also consistent with the muted trace metal enrichments predicted for

Emerging Topics in Life Sciences (2018)
https://doi.org/10.1042/ETLS20170163

shale deposited under a ferruginous water column. Thus, the role of the redox state in BST preservation remains controversial.

The Mural Formation: a test case

The Lower Cambrian (Series 2) Mural Formation, exposed in the southern Canadian Cordillera (Figure 1), offers an opportunity to refine our understanding of the role of redox state in BST preservation. In terms of preservation, the Mural Formation contains elements of BST soft-bodied preservation in one known locality near Mumm Peak (Figures 1 and 2D,E), but compared with Tier 1 and 2 biotas such as the Burgess Shale, Sirius Passet, Emu Bay or Chengjiang, it is by no means 'exceptional' in terms of abundance or preservational fidelity. In essence, it preserves recalcitrant cuticles rather than fine morphologies. Also in contrast with most BST deposits that were deposited well beneath the storm wave base [10], the Mural Formation shows evidence of storm activity in stratigraphic proximity to the beds with exceptional preservation. The Mural Formation therefore represents an endmember of BST preservation: perhaps deposited in slightly shallower water, and with soft-part preservation not seen in standard shelly faunas, but not as exceptional as the deservedly more famous BST deposits. In the classification of Gaines [10], this is a 'Tier 3' BST deposit (the worst level of fossil preservation). The goal of this study is to conduct a multi-proxy sedimentary geochemical study of the BST preservation interval in the Mural Formation — the first such study of a Tier 3 deposit — and compare the results with data obtained from other BST deposits worldwide. Overall, this work provides an important consistency test of existing hypotheses: if anoxia plays a central role in exceptional BST preservation, we would predict a more oxygenated signal in the Tier 3 Mural Formation than the investigated Tier 1 and 2 deposits.

Geological background

The Mural Formation was deposited during the early Cambrian Sauk transgression on the western Laurentian margin [52,53] and sits above the ~300–1700 m thick shallow-marine siliciclastics of the McNaughton Formation [54,55]. The McNaughton and overlying formations are generally thought to represent the rift-to-post-rift transition on the Laurentian margin [56,57], although continued syn-sedimentary faulting continued through the mid-Cambrian to the north. The Mural Formation is part of a broadly contiguous stratigraphic package spanning the *Nevadella–Bonnia/Olenellus* trilobite zones (Series 2; Waucoban) that stretches from Mexico to Yukon, Canada [52]. This package consists of an upper and lower carbonate composed of ooid grainstone shoals and archaeocyath bioherms, separated by a medial shale/siltstone (Figure 3).

The Mural Formation has been the subject of paleontological investigation for more than a century (primarily at its type section near Mumm Peak, Jasper National Park, the focus of study here), and workers have described an abundant shelly fauna including trilobites and obollelid and linguliform brachiopods [58–63]. Two known levels have also yielded soft-part preservation (Figure 3), the '*Lingulosacculus* quarry' that preserves soft-shelled brachiopods [64] (Figure 2E), and the 'waterfall quarry' level which contains as-yet undescribed vetulicolians, palaeoscolecid worms and anomalocarid appendages (Figure 2D). These soft-bodied preservation levels are located in gray, laminated shales between packages of shale containing beds and lenses of detrital carbonates, sometimes consisting of fossil hash. Whether these storm beds represent a shallowing into storm wave base during base-level change (i.e. parasequences) or occasional storm beds at a constant depth could not be determined, but in either case this represents a proximity to wave base not seen in Tier 1 and 2 BST deposits [10]. The Mural Formation does not display bioturbation through the medial shale.

Materials and methods

Twenty-seven shale samples were collected from the Mural Formation, all from the medial shale at the type section, and crushed in a tungsten carbide shatterbox. Total organic carbon (TOC) weight percent was analyzed on decalcified residue on a Carlo-Erba NA 1500 Elemental Analyzer. Weight percent iron in pyrite (FeP) was quantified using the chromium reducible sulfur method of Canfield et al. [65], and iron present in iron oxides, iron carbonates and magnetite was quantified using the sequential extraction method of Poulton and Canfield [66]. Precision estimates for these methods can be found in Supplementary Materials of refs [35,40]. Major, minor and trace element concentrations were analyzed by Bureau Veritas, Ltd, using ICP-MS/ICP-OES following multi-acid digestion. Aliquots of the USGS shale standards SBC-1 and SGR-1 were sent blind along with samples, and results were consistent with published values.

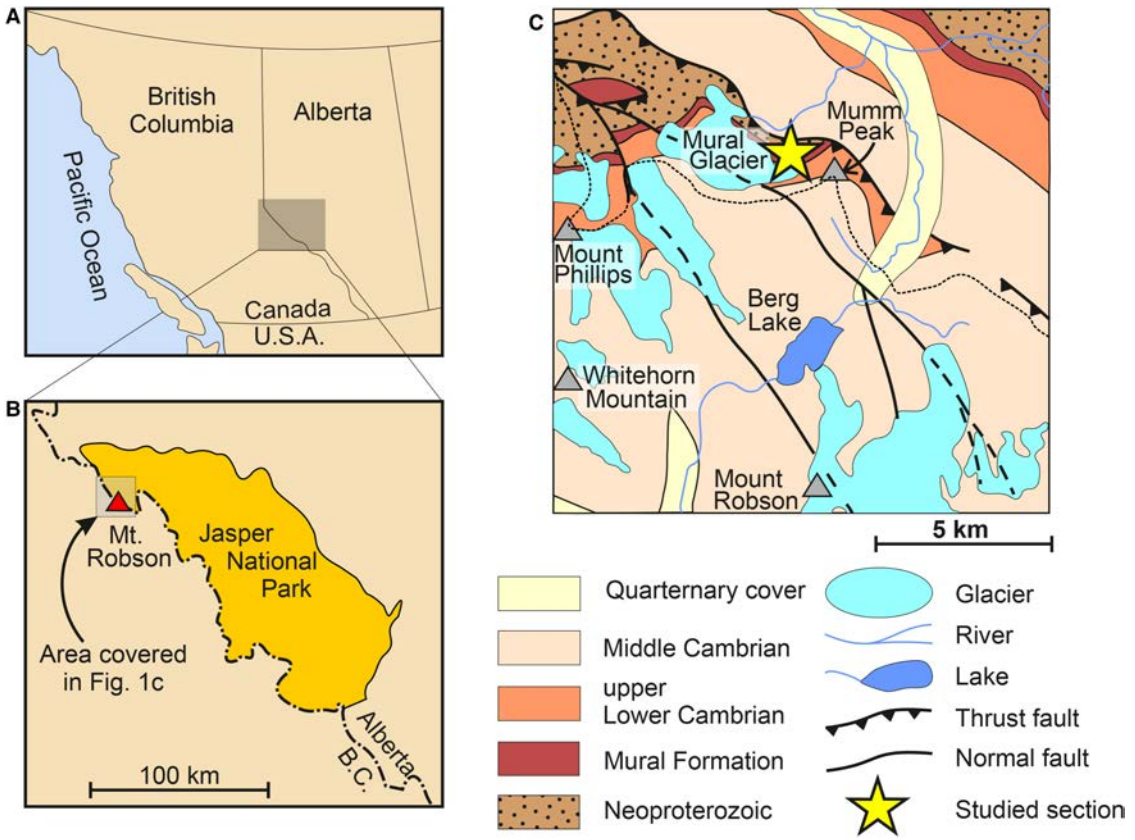

Figure 1. Geographic position of the Mural Formation section studied here. (**A-C**) Geological map of the study region, after GSC Map 1499A [93] and modified from ref. [62].

Results and discussion

All geochemical results are plotted in Figure 3 and reported in Supplementary Table S1. TOC weight percents in the Mural Formation are relatively low, at 0.14 ± 0.03 (1 SD). This probably rules out very high original sedimentary TOC values (as this signature can be retained even in the face of metamorphism, e.g. [67]), but as these are outcrop samples from a region that has experienced prehnite–pumpellyite grade (CAI of 3–5) metamorphism [68], the original TOC richness is unknown and certainly higher. Redox-sensitive trace metal contents are uniformly low and around crustal/average shale values. Specifically, Mo contents are all <1 ppm, U contents are 2.6 ± 0.4 ppm and V contents are 88 ± 8 ppm. As aluminum, a conservative tracer of detrital input, is also near or even slightly elevated compared with average shale values (9.4 ± 0.5 weight percent), the low redox-sensitive trace metal contents in the Mural cannot be explained by dilution by carbonates or other non-clastic material. Trace metal data are plotted in Figure 3 as enrichment factors (EFs), which is a method of accounting for the expected detrital metal input based on observed levels of a biogeochemically conservative element such as aluminum (discussed in ref. [28]). Values >>1 would indicate authigenic enrichment (due to reducing conditions). Values ~1 generally indicate the operation of purely detrital processes and oxic conditions. However, since there is so much possible variability in detrital input [41], and substantial authigenic metal enrichments might also not develop during rapid sedimentation, recognizing whether there have actually been slight enrichments or depletions is difficult to tell. The Mural Formation data unfortunately fall in this zone. Thus, like many other BST deposits investigated to date, the Mural Formation trace metal data rule out euxinic conditions but are consistent with either an oxic (no enrichment) or ferruginous (possibly muted enrichment) water column during deposition.

The iron geochemistry of the Mural Formation, though, differs from that of investigated BST deposits. FeHR/FeT values are low (0.17 ± 0.04), with all of the values being well below the 0.38 ratio usually taken as

Emerging Topics in Life Sciences (2018)
https://doi.org/10.1042/ETLS20170163

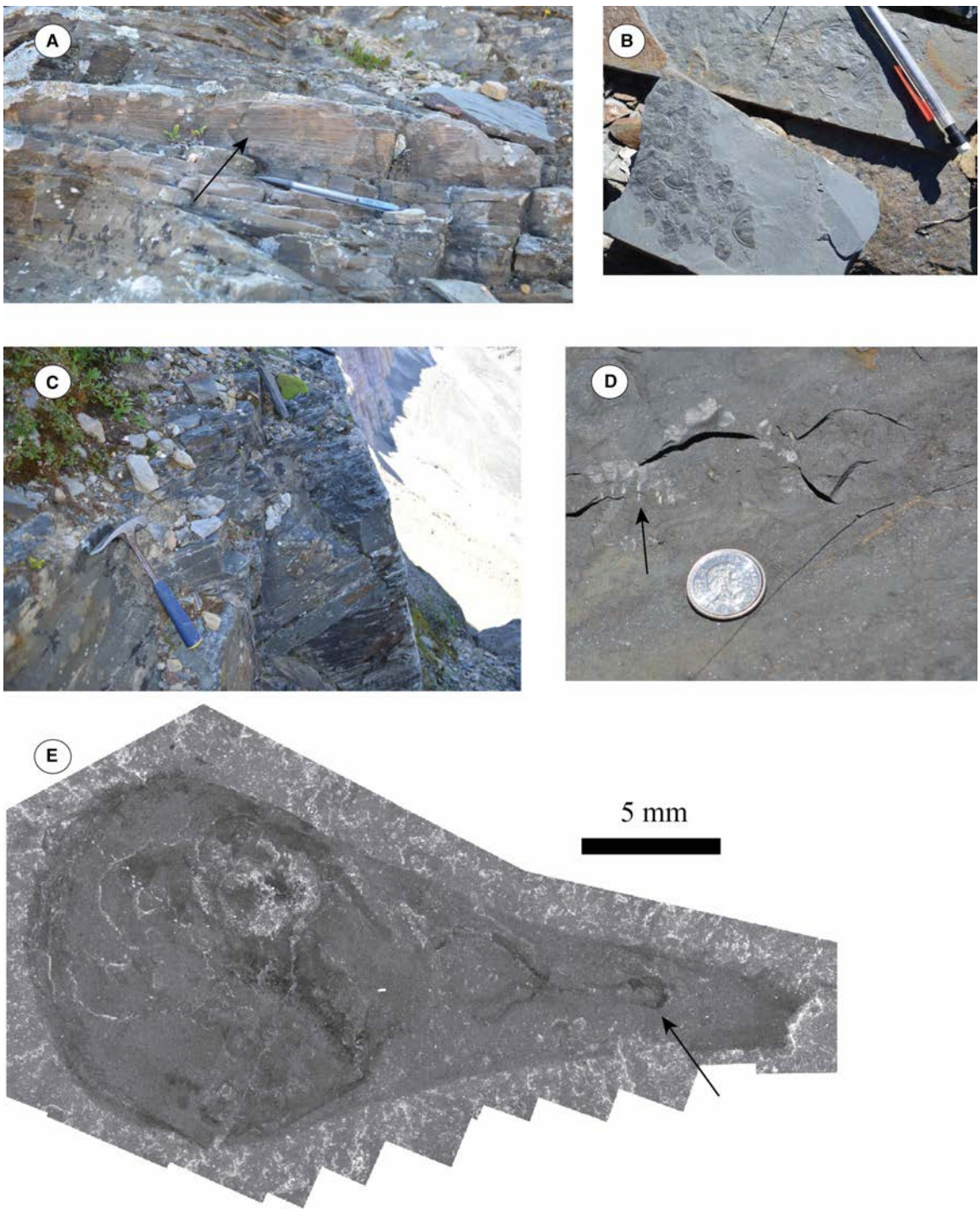

Figure 2. Sedimentology and paleontology of the medial shale/siltstone of the Mural Formation near Mumm Peak.
(**A**) Unlike exquisitely preserved Tier 1 and 2 BST deposits, the medial shale contains beds and lenses of detrital carbonate with indications of wave or current activity, such as cross beds (arrow). Photo from 107.4 m; mechanical pencil for scale. (**B**) Shale beds immediately adjacent to beds with current structures have a shelly fauna, with evidence of transport, such as this cluster of trilobite cephalons. Photo from local float at 117 m, mechanical pencil for scale. (**C**) The lower half of the medial shale also contains laminated gray shale intervals, such as this photo spanning ~114–115 m, at the 'waterfall quarry' level. 30 cm geological hammer for scale. These intervals host rare soft-bodied preservation. (**D**) *In situ* fragment of an anomalocarid claw (arrow), from 114 m (within 'waterfall quarry'); diameter of the Canadian quarter is 24 mm. (**E**) *Lingulosacculus nuda* [64] with a preserved gut trace (arrow), from '*Lingulosacculus* quarry' at 118.2–118.6 m. 5 mm scale bar on photo.

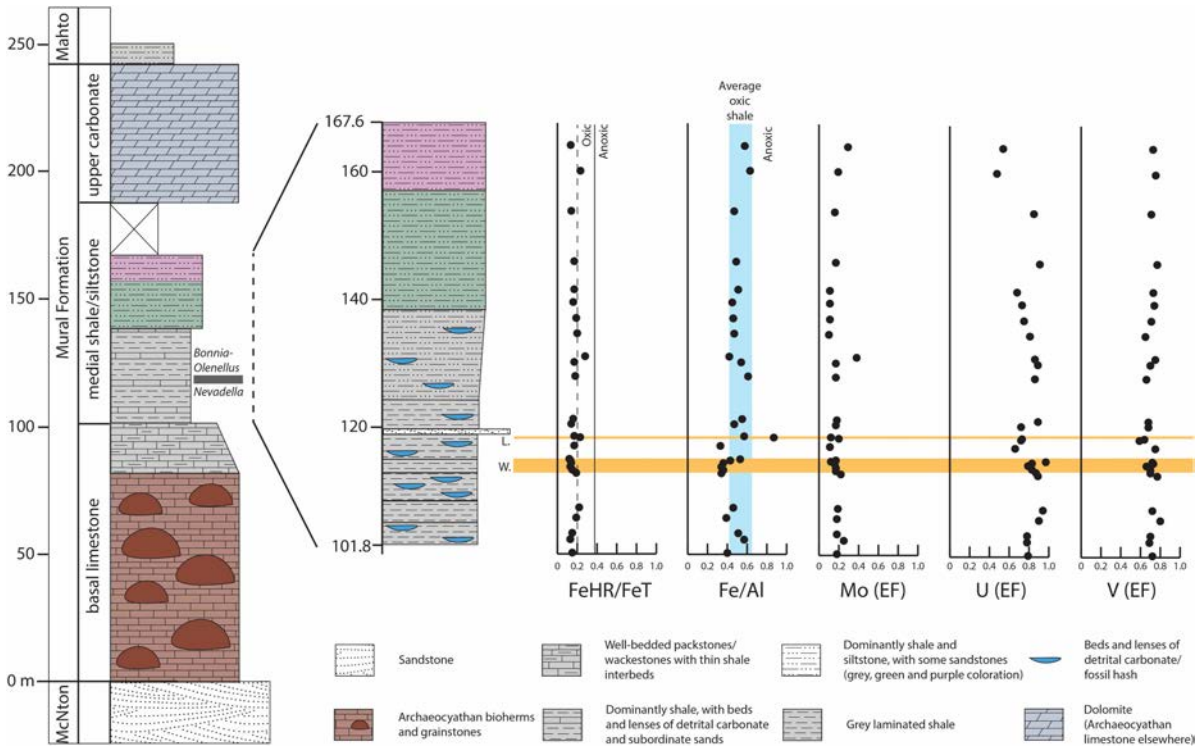

Figure 3. Lithostratigraphy and sedimentary geochemistry of the Mural Formation at Mumm Peak.

Total measured thickness of the Formation is very similar to that of ref. [59], but the heights of internal units differ slightly. *Nevadella–Bonnia/Olenellus* boundary is resolved to a 3.85 m interval between 117.3 and 121.15 m. Inset shows expanded stratigraphy of medial shale/siltstone. Geochemical data from left to right: (1) the iron speciation proxy (FeHR/FeT). Values above the vertical 0.38 line probably represent deposition under an anoxic water column, based on calibrations from the modern ocean [25]. Oxic sediment samples in the modern fall below this line, but anoxic samples can too, for instance, during turbiditic sedimentation. The dashed 0.2 line represents the lowest modern value for an anoxic turbiditic sediment [27]. FeP/FeHR values not graphed as all samples show an oxic signature; the average is 0.29 ± 0.15 (Supplementary Table S1). (2) Fe/Al ratio, with shaded blue bar representing the range of values seen in ancient oxic shale [72]. Values above this bar would indicate iron enrichment due to an anoxic water column. (3) Molybdenum EF. (4) Uranium EF. (5) Vanadium EF. For these samples, an EF of 1 represents an aluminum-normalized value equal to upper continental crust [30]. Values above 1 indicate enrichment, although recognition of muted enrichments/depletions can be difficult due to variations in detrital input [41]. Enrichment would be expected under an anoxic water column [28], yet all of these samples are unenriched. Abbreviations: McNton., McNaughton Formation; W., 'waterfall quarry' level from 112.8 to 114.9 m; L., '*Lingulosacculus* quarry' from 118.2 to 118.6 m.

indicative of an anoxic water column. The most straightforward explanation of these data is oxic deposition. However, it has been recognized that (1) fingerprinting anoxia is generally more straightforward than oxic conditions [37,69] and (2) there are many factors that can result in low FeHR enrichment (rapid deposition and source area effects) or drive FeHR/FeT values lower (metamorphism). Regarding rapid deposition, the medial shale does not have consistent sedimentological indicators of such processes, although it should be noted that obvious sedimentary structures are difficult to see in the outcrop. There is evidence for event-driven sedimentation in a relatively thick sandstone marker bed right above the exceptionally preserved interval. Considering that almost all BST deposits involve event-based sedimentation [10], a more detailed sedimentological and petrographic study of the Mural Formation may reveal additional evidence of these processes. Nonetheless, the observed FeHR/FeT values are still generally lower than the lowest 0.2 ratio recognized in the modern ocean for anoxic turbidites [27], suggesting a most parsimonious interpretation of oxic conditions even with respect to this caveat. Second, in some cases there may not be an appropriate source of detrital iron available to be shuttled into the anoxic basin, and it is this shuttle that ultimately generates the iron enrichments this proxy

Emerging Topics in Life Sciences (2018)
https://doi.org/10.1042/ETLS20170163

targets (discussed in ref. [69]). However, settings where this caveat matters are relatively rare, and stratigraphically underlying anoxic Neoproterozoic strata exhibit obvious iron enrichments [36]. Perhaps the most important consideration for the Mural is that highly reactive iron can be converted into poorly reactive iron during metamorphism, removing the evidence for anoxic sedimentation [26,70]. Fortunately, total iron (relative to aluminum) is also generally enriched by the iron shuttle under anoxic water columns [71,72], and this ratio is not as strongly affected by metamorphism. With the exception of one sample (interestingly, at the level of the *Lingulosacculus* quarry; Figure 3), the Fe/Al values (0.48 ± 0.11) are exactly within the range expected of oxic sediments [72]. In summary, although we cannot unambiguously rule out anoxic conditions, we can state (1) the only possible anoxic signal — in just one of multiple proxies — occurs at one of the soft-bodied preservation levels and (2) all other available evidence points toward the presence of at least some oxygen in the water column (or more precisely, provides no evidence for anoxia).

The Mural Formation thus preserves elements of BST biotas and has no evidence for anoxia. Although seemingly paradoxical, we argue that this provides strong evidence for the role of anoxic or periodically anoxic conditions in BST preservation. Put simply, the preservation in the Mural Formation is nowhere near that in the celebrated BST deposits. There is no exquisite, high-fidelity preservation of nervous systems, eyes, gut details and gills as in other deposits [73–76]. The fossils preserved in the Mural Formation at Mumm Peak are the recalcitrant endmembers of BST preservation: soft-shelled brachiopods [64] and anomalocarid appendages. Exceptionally preserved fossils in the Mural Formation are also rare and of low diversity; despite extensive quarrying during our fieldwork, we did not uncover new taxa that had not been found by previous field parties.

When comparing between BST deposits, it is worth noting that the overall differences in redox state may have been slight. For instance, the Mural is not extensively burrowed, suggesting that the water column was not fully oxygenated. Furthermore, some of the other more spectacular BST deposits may have been deposited in conditions that rapidly alternated between dysoxic and anoxic/ferruginous conditions, with the chemocline established perhaps only slightly above the sediment–water interface [24]. However, even considering the known difficulty of tracking low-oxygen conditions with available geochemical proxies [77], it is apparent that exceptional BST deposits (Tier 1 and 2) have a much greater prevalence of anoxic iron speciation signatures and/or total iron enrichments, minor but observable trace metal enrichments, and positive nitrogen isotope values [35,42,43,45] than the Mural Formation. In other words, there is now geochemical evidence suggesting that both the Mural Formation and the transition between the upper Maotianshan Shale and Yuanshan Member 3 in the Chengjiang deposit [43] were more oxygenated and 'decay-limited' than Tier 1 and 2 deposits. This supports previous analyses based on detailed sedimentological and ichnological studies that preservation in BST deposits was facilitated by anoxic conditions [24].

Toward a refined geochemical model

Moving forward, it is clear that anoxia was probably involved in preserving BST fossils, but it is also clear from both sedimentological/ichnological approaches [24,78,79] and multi-proxy geochemical studies [43,45] that these deposits were near the edge of the chemocline, with often-times rapid fluctuations into low-oxygen (suboxic/dysoxic) conditions. Tracking low oxygen levels is difficult with our current geochemical toolkit [77], and furthermore, the ecological/oceanographic timescales that matter for organismal habitat viability and fossil preservation often differ from the integrated longer-term geochemical signals studied in hand samples collected by geochemists [27]. Indeed, no published multi-proxy BST dataset is completely unambiguous; such ambiguity may actually be a hallmark of very low-oxygen or fluctuating oxic/anoxic systems. In light of this, further gains in understanding of the role of redox conditions will require new approaches. These may include increased efforts to obtain unoxidized drill cores (packsack or 'winky' drills may offer an alternative to a full drill rig; e.g. [80]), and moving from standard bulk-rock geochemistry (such as in this study) to increased micron- and phase-specific interrogation of the geochemical signal, especially in more metamorphosed deposits. Shale-based proxies that can unambiguously resolve oxygenated conditions would also be a major step forward.

Most important, geochemical studies should strive toward a multi-proxy approach incorporating as many sources of data as possible, but especially pairing redox-sensitive trace metal analysis with iron speciation. The recognition that water columns were commonly ferruginous (non-euxinic) during this time interval will often

make interpretation of trace metal data more difficult. Low Mo abundances are helpful in ruling out fully euxinic water columns [81,82], but in the absence of iron speciation data (the best available method for fingerprinting anoxic but non-euxinic conditions), low concentrations of elements like U, V and Cr are inconclusive as they could indicate either oxic or ferruginous conditions. Like the Mural Formation, some other 'Tier 3' Lagerstätte such as Indian Springs might have been deposited under an oxic water column [50], but this cannot be determined from trace metal data alone. A further issue lies in choosing baseline values. Many studies compare redox-sensitive trace metal data with the interpretive scheme of Jones and Manning [51]. This study was groundbreaking in its time (especially the cross-validation approach), but current consensus is that the scheme is optimistic in its true ability to detect such subtle redox shifts. Redox-sensitive trace metal behavior in sediments and the water column is complicated, and many of the Jones and Manning proxies (e.g. V/(V + Ni), Ni/Co or V/Cr) take two elements, each with incompletely understood redox properties and perhaps different detrital influences, and combine them together. The sum here is probably less than the parts. In light of this, we propose abandoning the Jones and Manning framework. Nuanced understanding of redox patterns with trace metals remains possible, but this should come through a careful comparative study of metal data as single-element EFs or metal/aluminum ratios (while paying heed to possible variation in detrital inputs [41]) and with respect to modern chemical oceanographic studies.

How exactly anoxic (or fluctuating anoxic-to-dysoxic) conditions directly affected BST preservation remains unclear. On the one hand, anoxia is a necessary but insufficient prerequisite for BST preservation by eliminating scavenging [10,19,21]. Early calcium carbonate cementation and low oceanic sulfate levels may have been equally important in sealing beds from oxidant delivery and reducing microbial decay [83]. Beyond simply considering 'anoxia', it may actually be the specific flavors of anoxia in the sediment and water column that are important in controlling preservation. Specifically, 'suboxic' microbial processes such as iron and manganese reduction dramatically increase alkalinity relative to dissolved inorganic carbon (DIC) and thus raise the calcium carbonate saturation state of porewaters. In contrast, sulfate reduction increases alkalinity approximately equal to DIC, and moves the saturation state along lines of roughly equal values (Ω) [84]. Enhanced iron reduction in Cambrian sediments could therefore have helped induce precipitation of the observed BST seafloor cements critical for 'sealing' carcasses in the sediment. It is worth noting here that many, but not all, of the BST cement layers carry a dominant seawater (rather than microbial) carbon isotope signature [83]. However, a seawater carbon signature can also be found in other carbonate precipitates believed to be triggered by 'suboxic' microbial metabolisms [84]. Essentially, a dominantly seawater carbon isotope signature does not negate a role for iron reduction, but rather suggests that relatively little microbial respiratory work was required to tip the scales and induce precipitation [84].

The fact that there was abundant iron reduction relative to sulfate reduction during early diagenesis in BST deposits has recently been demonstrated by clay mineralogy studies. A recent investigation of 19 Cambrian sedimentary successions on four continents found that BST deposits were highly correlated with the presence of iron-rich clay minerals (berthierine and chamosite) compared with deposits only containing shelly fossils [85]. These clays form during early diagenesis by the transformation of detrital clays in the presence of elevated porewater Fe^{2+}. The exact role of these clays in preservation is unclear, specifically whether they are simply a symptom of some other factor important in BST preservational pathways, or a cause [86,87]. Certainly, clays appear to function as antimicrobial agents in decay experiments [88], but the action of iron-rich clays is not significantly different from precursors like kaolinite, and the timescale for the formation of berthierine and chamosite is longer than the timescale required for labile tissue preservation. In any case, considering that porewater Fe^{2+} will not accumulate in the presence of sulfide [89], it is significant that anoxic Cambrian water columns *and* sediments appear to have had relatively low sulfide-generating potential [35]. Thus, a transition in the uppermost sediment column away from extensive iron reduction, and toward sulfate reduction (such as we see in modern OMZs), over the early Phanerozoic may have played multiple geochemical roles in the disappearance of BST preservation. In this view, a transition toward more oxygenated oceans with time may have been important [18], but this alone would be too simplistic; the relative rates of iron versus sulfate reduction matter too. In other words, as oxygen and sulfate levels rose through the Paleozoic [90,91], changes in sediments and water columns toward either more oxic or more sulfidic conditions may have inhibited BST preservational pathways. Most probably, the Burgess Shale-type taphonomic window was propped open by a 'perfect storm' of geochemical parameters in the Cambrian ocean [18,83,86,92].

Summary

- Poor preservation in Burgess Shale-type (BST) deposits is linked to relatively more oxygenated conditions, suggesting that anoxia probably played a role in the most exceptionally preserved deposits.

- The relative dominance of iron reduction compared with sulfate reduction in Cambrian sediments and water columns may have played a key role in factors required for BST preservation.

Abbreviations

BST, Burgess Shale-type; FeHR, highly reactive iron; DIC, dissolved inorganic carbon; EF, enrichment factors; FeP, iron in pyrite; FeT, total iron; ICP-MS, inductively coupled plasma mass spectrometry; ICP-OES, inductively coupled optical emission spectrometry; OMZs, oxygen minimum zones; TOC, total organic carbon.

Acknowledgements

We thank Una Farrell, Austin Miller, David Mucciarone and Douglas Turner for laboratory assistance, Jen Wasylyk at Parks Canada for help with permits and logistics, Jakob Vinther for field assistance, Richard Stockey, Emma Hammarlund, and Ross Anderson for helpful discussion, and Bob Gaines and an anonymous reviewer for formal comments. We thank Yellowhead helicopters for safe flying. We gratefully acknowledge support by the National Geographic Society's Global Exploration Fund — Northern Europe GEFNE113–14 and National Science Foundation grant DEB-1747731 to EAS.

Competing Interests

The Authors declare that there are no competing interests associated with the manuscript.

References

1 Erwin, D.H., Laflamme, M., Tweedt, S.M., Sperling, E.A., Pisani, D. and Peterson, K.J. (2011) The Cambrian conundrum: early divergence and later ecological success in the early history of animals. *Science* **334**, 1091–1097 https://doi.org/10.1126/science.1206375

2 Droser, M.L., Gehling, J.G. and Jensen, S. (1999) When the worm turned: concordance of Early Cambrian ichnofabric and trace-fossil record in siliclastic rocks of South Australia. *Geology* **27**, 625–628 https://doi.org/10.1130/0091-7613(1999)027<0625:WTWTCO>2.3.CO;2

3 Droser, M.L. and Bottjer, D.J. (1988) Trends in depth and extent of bioturbation in Cambrian carbonate marine environments, western United States. *Geology* **16**, 233–236 https://doi.org/10.1130/0091-7613(1988)016<0233:TIDAEO>2.3.CO;2

4 Buatois, L.A., Mángano, M.G., Olea, R.A. and Wilson, M.A. (2016) Decoupled evolution of soft and hard substrate communities during the Cambrian Explosion and Great Ordovician biodiversification event. *Proc. Natl Acad. Sci. U.S.A.* **113**, 6945–6948 https://doi.org/10.1073/pnas.1523087113

5 Porter, S.M. (2004) Closing the phosphatization window: testing for the influence of taphonomic megabias on the pattern of small shelly fossil decline. *Palaios* **19**, 178–183 https://doi.org/10.1669/0883-1351(2004)019<0178:CTPWTF>2.0.CO;2

6 Smith, E.F., Macdonald, F.A., Petach, T.A., Bold, U. and Schrag, D.P. (2016) Integrated stratigraphic, geochemical, and paleontological late Ediacaran to early Cambrian records from southwestern Mongolia. *Geol. Soc. Am. Bull* **128**, 442–468 https://doi.org/10.1130/B31248.1

7 Maloof, A.C., Porter, S.M., Moore, J.L., Dudas, F.O., Bowring, S.A., Higgins, J.A. et al. (2010) The earliest Cambrian record of animals and ocean geochemical change. *Geol. Soc. Am. Bull* **122**, 1731–1774 https://doi.org/10.1130/B30346.1

8 Butterfield, N. and Harvey, T. (2012) Small carbonaceous fossils (SCFs): a new measure of early Paleozoic paleobiology. *Geology* **40**, 71–74 https://doi.org/10.1130/G32580.1

9 Harvey, T.H.P., Vélez, M.I. and Butterfield, N.J. (2012) Exceptionally preserved crustaceans from western Canada reveal a cryptic Cambrian radiation. *Proc. Natl Acad. Sci. U.S.A.* **109**, 1589–1594 https://doi.org/10.1073/pnas.1115244109

10 Gaines, R.R. (2014) Burgess shale-type preservation and its distribution in space and time. *Paleontol. Soc. Pap.* **20**, 123–146

11 Sperling, E.A. (2013) Tackling the 99%: can we begin to understand the paleoecology of the small and soft-bodied animal majority? In *Ecosystem Paleobiology and Geobiology* (Bush, A.M., Pruss, S.B. and Payne, J.L., eds), pp. 77–86, Paleontological Society

12 Conway Morris, S.C. (1986) The community structure of the Middle Cambrian Phyllopod Bed (Burgess Shale). *Palaeontology* **29**, 427–467

13 Briggs, D.E.G. (2015) Extraordinary fossils reveal the nature of Cambrian life: a commentary on Whittington (1975) 'The enigmatic animal Opabinia regalis, Middle Cambrian, Burgess Shale, British Columbia'. *Philos. Trans. R. Soc. Lond. B. Biol. Sci.* **370**, 20140313 https://doi.org/10.1098/rstb.2014.0313

14 Briggs, D.E.G. (1991) Extraordinary fossils. *Am. Sci* **79**, 130–141

15 Caron, J.-B. and Jackson, D.A. (2008) Paleoecology of the Greater Phyllopod Bed community, Burgess shale. *Palaeogeogr. Palaeoclimatol. Palaeoecol.* **258**, 222–256 https://doi.org/10.1016/j.palaeo.2007.05.023

16 Briggs, D.E.G. and Fortey, R.A. (2005) Wonderful strife: systematics, stem groups, and the phylogenetic signal of the Cambrian radiation. *Paleobiology* **31**, 94–112 https://doi.org/10.1666/0094-8373(2005)031[0094:WSSSGA]2.0.CO;2

17 Allison, P.A. and Briggs, D.E.G. (1993) Exceptional fossil record: distribution of soft-tissue preservation through the Phanerozoic. *Geology* **21**, 527–530 https://doi.org/10.1130/0091-7613(1993)021<0527:EFRDOS>2.3.CO;2
18 Muscente, A.D., Schiffbauer, J.D., Broce, J., Laflamme, M., O'Donnell, K., Boag, T.H. et al. (2017) Exceptionally preserved fossil assemblages through geologic time and space. *Gondwana Res.* **48**, 164–188 https://doi.org/10.1016/j.gr.2017.04.020
19 Allison, P.A. (1988) The role of anoxia in the decay and mineralization of proteinaceous macro-fossils. *Paleobiology* **14**, 139–154 https://doi.org/10.1017/S009483730001188X
20 Hammarlund, E., Canfield, D.E., Bengtson, S., Leth, P.M., Schillinger, B. and Calzada, E. (2011) The influence of sulfate concentration on soft-tissue decay and preservation. *Palaeontogr. Can.* **31**, 141–156
21 Skinner, E.S. (2005) Taphonomy and depositional circumstances of exceptionally preserved fossils from the Kinzers Formation (Cambrian), southeastern Pennsylvania. *Palaeogeogr. Palaeoclimatol. Palaeoecol.* **220**, 167–192 https://doi.org/10.1016/j.palaeo.2004.09.015
22 Briggs, D.E.G. (2003) The role of decay and mineralization in the preservation of soft-bodied fossils. *Annu. Rev. Earth Planet. Sci.* **31**, 275–301 https://doi.org/10.1146/annurev.earth.31.100901.144746
23 Naimark, E., Kalinina, M. and Boeva, N. (2018) Persistence of external anatomy of small crustaceans in a long term taphonomic experiment. *Palaios* **33**, 154–163 https://doi.org/10.2110/palo.2017.083
24 Gaines, R.R. and Droser, M.L. (2010) The paleoredox setting of Burgess Shale-type deposits. *Palaeogeogr. Palaeoclimatol. Palaeoecol.* **297**, 649–661 https://doi.org/10.1016/j.palaeo.2010.09.014
25 Raiswell, R. and Canfield, D.E. (1998) Sources of iron for pyrite formation in marine sediments. *Am. J. Sci.* **298**, 219–245 https://doi.org/10.2475/ajs.298.3.219
26 Poulton, S.W. and Canfield, D.E. (2011) Ferruginous conditions: a dominant feature of the ocean through Earth's history. *Elements* **7**, 107–112 https://doi.org/10.2113/gselements.7.2.107
27 Sperling, E.A., Carbone, C., Strauss, J.V., Johnston, D.T., Narbonne, G.M. and Macdonald, F.A. (2016) Oxygen, facies, and secular controls on the appearance of Cryogenian and Ediacaran body and trace fossils in the Mackenzie Mountains of northwestern Canada. *Geol. Soc. Am. Bull.* **128**, 558–575 https://doi.org/10.1130/B31329.1
28 Tribovillard, N., Algeo, T.J., Lyons, T. and Riboulleau, A. (2006) Trace metals as paleoredox and paleoproductivity proxies: an update. *Chem. Geol.* **232**, 12–32 https://doi.org/10.1016/j.chemgeo.2006.02.012
29 Turekian, K.K. and Wedepohl, K.H. (1961) Distribution of the elements in some major units of the earth's crust. *Geol. Soc. Am. Bull.* **72**, 175–192 https://doi.org/10.1130/0016-7606(1961)72[175:DOTEIS]2.0.CO;2
30 McLennan, S.M. (2001) Relationships between the trace element composition of sedimentary rocks and upper continental crust. *Geochem. Geophys. Geosyst.* **2**, 1021 https://doi.org/10.1029/2000GC000109
31 Helz, G.R., Miller, C.V., Charnock, J.M., Mosselmans, J.F.W., Pattrick, R.A.D., Garner, C.D. et al. (1996) Mechanism of molybdenum removal from the sea and its concentration in black shales: EXAFS evidence. *Geochim. Cosmochim. Acta* **60**, 3631–3642 https://doi.org/10.1016/0016-7037(96)00195-0
32 Erickson, B.E. and Helz, G.R. (2000) Molybdenum(VI) speciation in sulfidic waters: stability and lability of thiomolybdates. *Geochim. Cosmochim. Acta* **64**, 1149–1158 https://doi.org/10.1016/S0016-7037(99)00423-8
33 Wanty, R.B. and Goldhaber, M.B. (1992) Thermodynamics and kinetics of reactions involving vanadium in natural systems: accumulation of vanadium in sedimentary rocks. *Geochim. Cosmochim. Acta* **56**, 1471–1483 https://doi.org/10.1016/0016-7037(92)90217-7
34 Guilbaud, R., Poulton, S.W., Butterfield, N.J., Zhu, M. and Shields-Zhou, G.A. (2015) A global transition to ferruginous conditions in the early Neoproterozoic oceans. *Nat. Geosci.* **8**, 466–470 https://doi.org/10.1038/ngeo2434
35 Sperling, E.A., Wolock, C.J., Morgan, A.S., Gill, B.C., Kunzmann, M., Halverson, G.P. et al. (2015) Statistical analysis of iron geochemical data suggests limited late Proterozoic oxygenation. *Nature* **523**, 451–454 https://doi.org/10.1038/nature14589
36 Canfield, D.E., Poulton, S.W., Knoll, A.H., Narbonne, G.M., Ross, G., Goldberg, T. et al. (2008) Ferruginous conditions dominated later Neoproterozoic deep-water chemistry. *Science* **321**, 949–952 https://doi.org/10.1126/science.1154499
37 Sperling, E.A., Rooney, A.D., Hays, L., Sergeev, V.N., Vorob'eva, N.G., Sergeeva, N.D. et al. (2014) Redox heterogeneity of subsurface waters in the Mesoproterozoic ocean. *Geobiology* **12**, 373–386 https://doi.org/10.1111/gbi.12091
38 Li, C., Planavsky, N.J., Love, G.D., Reinhard, C.T., Hardisty, D., Feng, L. et al. (2015) Marine redox conditions in the middle Proterozoic ocean and isotopic constraints on authigenic carbonate formation: insights from the Chuanlinggou Formation, Yanshan Basin, North China. *Geochim. Cosmochim. Acta* **150**, 90–105 https://doi.org/10.1016/j.gca.2014.12.005
39 Marz, C., Poulton, S.W., Beckmann, B., Kuster, K., Wagner, T. and Kasten, S. (2008) Redox sensitivity of P cycling during marine black shale formation: dynamics of sulfidic and anoxic, non-sulfidic bottom waters. *Geochim. Cosmochim. Acta* **72**, 3703–3717 https://doi.org/10.1016/j.gca.2008.04.025
40 Miller, A.J., Strauss, J.V., Halverson, G.P., MacDonald, F.A., Johnston, D.T. and Sperling, E.A. (2017) Tracking the onset of Phanerozoic-style redox-sensitive trace metal enrichments: new results from basal Ediacaran post-glacial strata in NW Canada. *Chem. Geol.* **457**, 24–37 https://doi.org/10.1016/j.chemgeo.2017.03.010
41 Cole, D.B., Zhang, S. and Planavsky, N.J. (2017) A new estimate of detrital redox-sensitive metal concentrations and variability in fluxes to marine sediments. *Geochim. Cosmochim. Acta* **215**, 337–353 https://doi.org/10.1016/j.gca.2017.08.004
42 Raiswell, R. and Canfield, D.E. (2012) The iron biogeochemical cycle past and present. *Geochem. Perspect.* **1**, 1–322 https://doi.org/10.7185/geochempersp.1.1
43 Hammarlund, E.U., Gaines, R.R., Prokopenko, M.G., Qi, C., Hou, X.-G. and Canfield, D.E. (2017) Early Cambrian oxygen minimum zone-like conditions at Chengjiang. *Earth Planet. Sci. Lett.* **475**, 160–168 https://doi.org/10.1016/j.epsl.2017.06.054
44 Kloss, T.J., Dornbos, S.Q., Chen, J.-Y., McHenry, L.J. and Marenco, P.J. (2015) High-resolution geochemical evidence for oxic bottom waters in three Cambrian Burgess Shale-type deposits. *Palaeogeogr. Palaeoclimatol. Palaeoecol.* **440**, 90–95 https://doi.org/10.1016/j.palaeo.2015.08.048
45 Hammarlund, E., Smith, M.P., Rasmussen, J., Nielsen, A., Canfield, D. and Harper, D. The Sirius Passet Lagerstätte of North Greenland — a geochemical window on early Cambrian low oxygen environments and ecosystems. *Geobiology*. in review
46 Powell, W.G., Johnston, P.A. and Collom, C.J. (2003) Geochemical evidence for oxygenated bottom waters during deposition of fossiliferous strata of the Burgess Shale Formation. *Palaeogeogr. Palaeoclimatol. Palaeoecol.* **201**, 249–268 https://doi.org/10.1016/S0031-0182(03)00612-6

47 Boudec, A.L., Ineson, J., Rosing, M., Døssing, L., Martineau, F., Lécuyer, C. et al. (2014) Geochemistry of the Cambrian Sirius Passet Lagerstätte, Northern Greenland. *Geochem. Geophys. Geosyst.* **15**, 886–904 https://doi.org/10.1002/2013GC005068
48 McKirdy, D.M., Hall, P.A., Nedin, C., Halverson, G.P., Michaelsen, B.H., Jago, J.B. et al. (2011) Paleoredox status and thermal alteration of the lower Cambrian (Series 2) Emu Bay Shale Lagerstätte, South Australia. *Aust. J. Earth Sci.* **58**, 259–272 https://doi.org/10.1080/08120099.2011.557439
49 Kimmig, J. and Pratt, B.R. (2016) Taphonomy of the middle Cambrian (Drumian) Ravens Throat River Lagerstätte, Rockslide Formation, Mackenzie Mountains, Northwest Territories, Canada. *Lethaia* **49**, 150–169 https://doi.org/10.1111/let.12135
50 Novek, J.M., Dornbos, S.Q. and McHenry, L.J. (2016) Palaeoredox geochemistry and bioturbation levels of the exceptionally preserved early Cambrian Indian Springs biota, Nevada, USA. *Lethaia* **49**, 604–616 https://doi.org/10.1111/let.12169
51 Jones, B. and Manning, D.A.C. (1994) Comparison of geochemical indices used for the interpretation of palaeoredox conditions in ancient mudstones. *Chem. Geol.* **111**, 111–129 https://doi.org/10.1016/0009-2541(94)90085-X
52 Pope, M.C., Hollingsworth, J.S. and Dilliard, K. (2012) Overview of Lower Cambrian mixed carbonate-siliciclastic deposition along the western Laurentian passive margin. In *The Great American Carbonate Bank: The Geology and Economic Resources of the Cambrian-Ordovician Suak Megasequence of Laurentia* (Derby, J.R., Fritz, R.D., Longacre, S.A., Morgan, W.A. and Stembach, C.A., eds), pp. 735–750, AAPG Memoir 98, AAPG (The American Association of Petroleum Geologists)
53 Pyle, L.J. (2012) Cambrian and Lower Ordovician Sauk megasequence of northwestern Canada, northern Rocky Mountains to the Beaufort Sea. In *The Great American Carbonate Bank: The Geology and Economic Resources of the Cambrian-Ordovician Sauk Megasequence of Laurentia* (Derby, J.R., Fritz, R.D., Longacre, S.A., Morgan, W.A. and Stembach, C.A., eds), pp. 675–723, AAPG Memoir 98.
54 Slind, O.L. and Perkins, G.D. (1966) Lower Paleozoic and Proterozoic sediments of the Rocky Mountains between Jasper, Alberta and Pine River, British Columbia. *Bull. Can. Pet. Geol.* **14**, 442–468
55 McMechan, M.E. (1990) Upper Proterozoic to Middle Cambrian history of the Peace River Arch: evidence from the Rocky Mountains. *Bull. Can. Pet. Geol.* **38**, 36–44
56 Bond, G.C., Christie-Blick, N., Kominz, M.A. and Devlin, W.J. (1985) An early Cambrian rift to post-rift transition in the Cordillera of western North America. *Nature* **315**, 742–746 https://doi.org/10.1038/315742a0
57 Lickorish, W.H. and Simony, P.S. (1995) Evidence for late rifting of the Cordilleran margin outlined by stratigraphic division of the Lower Cambrian Gog Group, Rocky Mountain Main Ranges, British Columbia and Alberta. *Can. J. Earth Sci.* **32**, 860–874 https://doi.org/10.1139/e95-072
58 Fritz, W.H. (1992) *Walcott's Lower Cambrian Olenellid Trilobite Collection 61K, Mount Robson Area, Canadian Rocky Mountains*, Geological Survey of Canada, Ottawa, Canada
59 Fritz, W.H. and Mountjoy, E.W. (1975) Lower and early Middle Cambrian formations near Mount Robson, British Columbia and Alberta. *Can. J. Earth Sci.* **12**, 119–131 https://doi.org/10.1139/e75-013
60 Walcott, C.D. (1913) New Lower Cambrian Subfauna. *Smithson Misc. Collect.* **57**, 309–326
61 Balthasar, U. (2008) Mummpikia Gen. Nov. and the origin of calcitic-shelled brachiopods. *Palaeontology* **51**, 263–279 https://doi.org/10.1111/j.1475-4983.2008.00754.x
62 Balthasar, U. (2004) Shell structure, ontogeny and affinities of the Lower Cambrian bivalved problematic fossil *Mickwitzia muralensis*. *Lethaia* **37**, 381–400 https://doi.org/10.1080/00241160410002090
63 Ortega-Hernández, J., Esteve, J. and Butterfield, N.J. (2013) Humble origins for a successful strategy: complete enrolment in early Cambrian olenellid trilobites. *Biol. Lett.* **9**, 20130679 https://doi.org/10.1098/rsbl.2013.0679
64 Balthasar, U. and Butterfield, N.J. (2009) Early Cambrian 'soft-shelled' brachiopods as possible stem-group phoronids. *Acta Palaeontol. Pol.* **54**, 307–314 https://doi.org/10.4202/app.2008.0042
65 Canfield, D.E., Raiswell, R., Westrich, J.T., Reaves, C.M. and Berner, R.A. (1986) The use of chromium reduction in the analysis of reduced inorganic sulfur in sediments and shale. *Chem. Geol.* **54**, 149–155 https://doi.org/10.1016/0009-2541(86)90078-1
66 Poulton, S.W. and Canfield, D.E. (2005) Development of a sequential extraction procedure for iron: implications for iron partitioning in continentally derived particulates. *Chem. Geol.* **214**, 209–221 https://doi.org/10.1016/j.chemgeo.2004.09.003
67 Anbar, A.D., Duan, Y., Lyons, T.W., Arnold, G.L., Kendall, B., Creaser, R.A. et al. (2007) A whiff of oxygen before the great oxidation event? *Science* **317**, 1903–1906 https://doi.org/10.1126/science.1140325
68 Read, P.B., Woodsworth, G.J., Greenwood, H.J., Ghent, E.D. and Evenchick, C.A. (1991) *Metamorphic map of the Canadian Cordillera. 'A' Series Map 1714A*, Geological Survey of Canada
69 Diamond, C.W., Planavsky, N.J., Wang, C. and Lyons, T.W. (2018) What the ~1.4 Ga Xiamaling Formation can and cannot tell us about the mid-Proterozoic ocean. *Geobiology* **16**, 219–236 https://doi.org/10.1111/gbi.12282
70 Slotznick, S.P., Eiler, J.M. and Fischer, W.W. (2018) The effects of metamorphism on iron mineralogy and the iron speciation redox proxy. *Geochim. Cosmochim. Acta* **224**, 96–115 https://doi.org/10.1016/j.gca.2017.12.003
71 Lyons, T.W. and Severmann, S. (2006) A critical look at iron paleoredox proxies: new insights from modern euxinic marine basins. *Geochim. Cosmochim. Acta* **70**, 5698–5722 https://doi.org/10.1016/j.gca.2006.08.021
72 Raiswell, R., Newton, R., Bottrell, S.H., Coburn, P.M., Briggs, D.E.G. Bond, D.P.G. et al. (2008) Turbidite depositional influences on the diagenesis of Beecher's Trilobite Bed and the Hunsrück Slate; sites of soft tissue pyritization. *Am. J. Sci.* **308**, 105–129 https://doi.org/10.2475/02.2008.01
73 Paterson, J.R., García-Bellido, D.C., Lee, M.S.Y., Brock, G.A., Jago, J.B. and Edgecombe, G.D. (2011) Acute vision in the giant Cambrian predator *Anomalocaris* and the origin of compound eyes. *Nature* **480**, 237–240 https://doi.org/10.1038/nature10689
74 Ma, X., Cong, P., Hou, X., Edgecombe, G.D. and Strausfeld, N.J. (2014) An exceptionally preserved arthropod cardiovascular system from the early Cambrian. *Nat. Commun.* **5**, 3560 https://doi.org/10.1038/ncomms4560
75 Ma, X., Hou, X., Edgecombe, G.D. and Strausfeld, N.J. (2012) Complex brain and optic lobes in an early Cambrian arthropod. *Nature* **490**, 258–261 https://doi.org/10.1038/nature11495
76 Butterfield, N.J. (2002) Leanchoilia guts and the interpretation of three-dimensional structures in Burgess Shale-type fossils. *Paleobiology* **28**, 155–171 https://doi.org/10.1666/0094-8373(2002)028<0155:LGATIO>2.0.CO;2

77 Boyer, D.L., Owens, J.D., Lyons, T.W. and Droser, M.L. (2011) Joining forces: combined biological and geochemical proxies reveal a complex but refined high-resolution palaeo-oxygen history in Devonian epeiric seas. *Palaeogeogr. Palaeoclimatol. Palaeoecol.* **306**, 134–146 https://doi.org/10.1016/j.palaeo.2011.04.012
78 Gaines, R.R. and Droser, M.L. (2003) Paleoecology of the familiar trilobite *Elrathia kingii*: an early exaerobic zone inhabitant. *Geology* **31**, 941–944 https://doi.org/10.1130/G19926.1
79 Garson, D.E., Gaines, R.R., Droser, M.L., Liddell, W.D. and Sappenfield, A. (2011) Dynamic palaeoredox and exceptional preservation in the Cambrian Spence Shale of Utah. *Lethaia*, **45**, 164–177.
80 Ahm, A.-S.C., Bjerrum, C.J. and Hammarlund, E.U. (2017) Disentangling the record of diagenesis, local redox conditions, and global seawater chemistry during the latest Ordovician glaciation. *Earth Planet. Sci. Lett.* **459**, 145–156 https://doi.org/10.1016/j.epsl.2016.09.049
81 Scott, C. and Lyons, T.W. (2012) Contrasting molybdenum cycling and isotopic properties in euxinic versus non-euxinic sediments and sedimentary rocks: refining the paleoproxies. *Chem. Geol.* **324**, 19–27 https://doi.org/10.1016/j.chemgeo.2012.05.012
82 Dahl, T.W., Ruhl, M., Hammarlund, E.U., Canfield, D.E., Rosing, M.T. and Bjerrum, C.J. (2013) Tracing euxinia by molybdenum concentrations in sediments using handheld X-ray fluorescence spectroscopy (HHXRF). *Chem. Geol.* **360**, 241–251 https://doi.org/10.1016/j.chemgeo.2013.10.022
83 Gaines, R.R., Hammarlund, E.U., Hou, X., Qi, C., Gabbott, S.E., Zhao, Y. et al. (2012) Mechanism for Burgess Shale-type preservation. *Proc. Natl Acad. Sci. U.S.A.* **109**, 5180–5184 https://doi.org/10.1073/pnas.1111784109
84 Bergmann, K.D., Grotzinger, J.P. and Fischer, W.W. (2013) Biological influences on seafloor carbonate precipitation. *Palaios* **28**, 99–115 https://doi.org/10.2110/palo.2012.p12-088r
85 Anderson, R.P., Tosca, N.J., Gaines, R.R., Koch, N.M. and Briggs, D.E.G. (2018) A mineralogical signature for Burgess Shale–type fossilization. *Geology* **46**, 2–5 https://doi.org/10.1130/G39941.1
86 Petrovich, R. (2001) Mechanisms of fossilization of the soft-bodied and lightly armored faunas of the Burgess Shale and of some other classical localities. *Am. J. Sci.* **301**, 683–726 https://doi.org/10.2475/ajs.301.8.683
87 Wilson, L.A. and Butterfield, N.J. (2014) Sediment effects on the preservation of Burgess shale-type compression fossils. *Palaios* **29**, 145–154 https://doi.org/10.2110/palo.2013.075
88 McMahon, S., Anderson, R.P., Saupe, E.E. and Briggs, D.E.G. (2016) Experimental evidence that clay inhibits bacterial decomposers: implications for preservation of organic fossils. *Geology* **44**, 867–870 https://doi.org/10.1130/G38454.1
89 Canfield, D.E. (1989) Reactive iron in marine sediments. *Geochim. Cosmochim. Acta* **53**, 619–632 https://doi.org/10.1016/0016-7037(89)90005-7
90 Lyons, T.W., Reinhard, C.T. and Planavsky, N.J. (2014) The rise of oxygen in Earth's early ocean and atmosphere. *Nature* **506**, 307–315 https://doi.org/10.1038/nature13068
91 Canfield, D.E. and Farquhar, J. (2009) Animal evolution, bioturbation, and the sulfate evolution of the oceans. *Proc. Natl Acad. Sci. U.S.A.* **106**, 8123–8127 https://doi.org/10.1073/pnas.0902037106
92 Lyons, T.W. (2012) A perfect (geochemical) storm yielded exceptional fossils in the early ocean. *Proc. Natl Acad. Sci. U.S.A.* **109**, 5138–5139 https://doi.org/10.1073/pnas.1202201109
93 Montjoy, E.W. (1980) *Geology, Mount Robson, West of Sixth Meridian ('A' Map Series Map 1499A)*, Geological Survey of Canada, Alberta, British Columbia